# Numerical simulation of flows around jellyfish in a current

\*T. Inomoto<sup>1</sup>, K. Matsuno<sup>2</sup>, M. Yamakawa<sup>2</sup>, S. Asao<sup>3</sup> and S. Ishihara<sup>1</sup>

<sup>1</sup>Graduate School of Science and Technology, Kyoto Institute of Technology, Matsugasaki, Sakyo-ku, Kyoto, Japan.
 <sup>2</sup>Department of Mechanical and Engineering, Kyoto Institute of Technology, Matsugasaki, Sakyo-ku, Kyoto, Japan.
 <sup>3</sup>Department of Mechanical Engineering, College of Industrial Technology, 1-27-1 Amagasaki, Hyogo, Japan.

\*Presenting and corresponding author: d3821501@edu.kit.ac.jp

#### **Abstract**

Coupled behaviors of fluid-flow and swimming-jellyfish are necessary for swimming movements and the dynamics governing these coupled behaviors is difficult and complex. A lot of researches investigated coupled behaviors of fluid-flow and jellyfish-swimming by using two-dimensional axisymmetric numerical simulations. However, in order to simulate swimming jellyfish in an asymmetric current, the three-dimensional simulation is necessary. On the other hand, in the simulation of an unsteady flow caused by a moving wall boundary, the Geometric Conservation Law (GCL) is important. In the computational method which does not strictly satisfy GCL, arbitrary grids moving affects the flow field and the physical conservation law is destroyed. Moving-Grid Finite-Volume Method (MGFVM) is suitable for such a flow because GCL is strictly satisfied. In MGFVM, GCL condition is automatically and strictly satisfied by the discretization performed using a four-dimensional control volume in the space and time unified domain (x, y, z, t). In this paper, we perform the three-dimensional coupled simulation of fluid-flow and jellyfish-swimming with six degrees of freedom of motion by using MGFVM and investigate the influence of a current on swimming jellyfish.

Keywords: Coupled simulation, Swimming, Jellyfish, Incompressible Flow

#### Introduction

Coupled behaviors of fluid-flow and swimming-jellyfish are necessary for swimming movements and the dynamics governing these behaviors is difficult and complex. Jellyfish were the earliest animals to evolve muscle-powered swimming in the sea. A swimming of jellyfish consists of contraction, relaxation and inertia. First swimming mechanism is a jet propulsion caused by the subumbrella volume change that occurs during the contraction and the relaxation. In a jet motion, a first vortex ring, which is called the 'starting vortex', occurs by the contraction and causes a strong jet propulsion. Second swimming mechanism is a paddling motion on the bell margin and not as simple as jet propulsion. In a paddling motion, a second vortex ring, which is called the 'stopping vortex', occurs by the relaxation. The stopping vortex rotates in the direction opposite to the starting vortex and influences the starting vortex. The stopping vortex plays an important role in swimming mechanisms [Colin and Costello (2002); Mchenry and Jed (2003); Dabiri et al. (2005); Costello et al. (2008)].

A lot of researches investigated swimming jellyfish by using computational fluid dynamics (CFD). The dynamics of swimming jellyfish was modeled by using the two-dimensional simulation using the SIMPLE algorithm [Dular et al. (2009)]. The vortex structure caused by a swimming jellyfish was investigated by using the two-dimensional simulation using the arbitrary Lagrangian–Eulerian (ALE) method [Sahin and Mohseni (2009)]. The relationship between kinematics and swimming jellyfish was investigated by using the two-dimensional axisymmetric simulation [Alben et al. (2013)]. The three-dimensional geometry of swimming jellyfish was extrapolated from the two-dimensional axisymmetric simulation [Rudolf and Mould (2010)]. Thus far, there are few investigations into three-

dimensional simulations of swimming jellyfish. Moreover, in these investigations, it was assumed that jellyfish is in stationary fluid. However, in the sea, a current may change the vortex structure caused by swimming jellyfish and affect a swimming of jellyfish. The swimming jellyfish in the current cannot be simulated by using a two-dimensional axisymmetric simulation because the current is not axisymmetric. Thus, a three-dimensional simulation is necessary in order to investigate the influence of the current on swimming jellyfish.

On the other hand, in the simulation of an unsteady flow caused by a moving wall boundary, the computational grid moves and deforms time-dependently. As the computational method for such a moving grid, the method applying discretization of the governing equation on a general bodyconforming curvilinear coordinate [Vinokur (1974)], the arbitrary Lagrangian-Eulerian (ALE) method in which the mesh point can be moved independently of fluid motion [Noh (1964)], the space-time finite-element method [Tezduvar et al. (1992)] and so on were suggested. It is most important for the computational method for moving grid that the Geometric Conservation Law (GCL) is satisfied [Thomas and Lombard (1979)]. In the computational method which does not strictly satisfy GCL, arbitrary grids moving may affect the flow field and physical conservation law may be destroyed. Moving-Grid Finite-Volume Method (MGFVM) was suggested as the computational method which strictly satisfy GCL [Mihara (1999)] and its performance was shown in various unsteady flows [Matsuno (2010)]. The GCL condition is automatically and strictly satisfied by the discretization performed using a four-dimensional control volume in the space and time unified domain (x, y, z, t). In structured grids, the method was firstly applied to compressible flows [Matsuno (2001)] and extended to incompressible flows [Inomoto (2004)]. In incompressible flows, the couple of pressure and velocity was done by the fractional step method on the four-dimensional domain. In order to apply to the object of complicated shape, Unstructured Moving-Grid Finite-Volume Method, which was MGFVM extended to unstructured grids, was suggested [Yamakawa and Matsuno (2003)]. Moreover, in order to apply to a greatly moving wall boundary, Moving Computational Domain (MCD) approach in which whole of computational region could move was suggested [Watanabe and Matsuno (2009)].

In this paper, we perform the three-dimensional coupled simulation of fluid-flow and jellyfish-swimming in a current with six degrees of freedom of motion by using Moving-Grid Finite-Volume Method. The swimming jellyfish demonstrated and the influence of the current is shown.

## Governing equations for fluid flow

Governing Equation

The governing equations of fluid-flow are the continuity equation,

$$\frac{\partial u}{\partial t} + \frac{\partial v}{\partial x} + \frac{\partial w}{\partial v} = 0,\tag{1}$$

and the Navier-Stokes equations for incompressible flow,

$$\frac{\partial \mathbf{q}}{\partial t} + \frac{\partial \mathbf{E}}{\partial x} + \frac{\partial \mathbf{F}}{\partial y} + \frac{\partial \mathbf{G}}{\partial z} + \frac{\partial \mathbf{P}_1}{\partial x} + \frac{\partial \mathbf{P}_2}{\partial y} + \frac{\partial \mathbf{P}_3}{\partial z} = 0,$$
(2)

with

$$\mathbf{E} = \mathbf{E}_{a} - \mathbf{E}_{v}, \quad \mathbf{F} = \mathbf{F}_{a} - \mathbf{F}_{v}, \quad \mathbf{G} = \mathbf{G}_{a} - \mathbf{G}_{v}, \quad \mathbf{q} = \begin{bmatrix} u \\ v \\ w \end{bmatrix}, \quad \mathbf{E}_{a} = \begin{bmatrix} u^{2} \\ uv \\ uw \end{bmatrix}, \quad \mathbf{F}_{a} = \begin{bmatrix} vu \\ v^{2} \\ vw \end{bmatrix}, \quad \mathbf{G}_{a} = \begin{bmatrix} wu \\ wv \\ w^{2} \end{bmatrix}, \quad \mathbf{E}_{v} = \frac{1}{\mathrm{Re}} \begin{bmatrix} \frac{\partial u}{\partial y} \\ \frac{\partial v}{\partial y} \\ \frac{\partial v}{\partial y} \end{bmatrix}, \quad \mathbf{G}_{v} = \frac{1}{\mathrm{Re}} \begin{bmatrix} \frac{\partial u}{\partial z} \\ \frac{\partial v}{\partial z} \\ \frac{\partial v}{\partial z} \end{bmatrix}, \quad \mathbf{P}_{1} = \begin{bmatrix} p \\ 0 \\ 0 \\ 0 \end{bmatrix}, \quad \mathbf{P}_{2} = \begin{bmatrix} 0 \\ p \\ 0 \\ 0 \end{bmatrix}, \quad \mathbf{P}_{3} = \begin{bmatrix} 0 \\ 0 \\ p \\ 0 \end{bmatrix}, \quad \mathbf{P}_{4} = \begin{bmatrix} 0 \\ 0 \\ 0 \\ 0 \end{bmatrix}, \quad \mathbf{P}_{5} = \begin{bmatrix} 0 \\ 0 \\ 0 \\ 0 \end{bmatrix}, \quad \mathbf{P}_{5} = \begin{bmatrix} 0 \\ 0 \\ 0 \\ 0 \end{bmatrix}, \quad \mathbf{P}_{5} = \begin{bmatrix} 0 \\ 0 \\ 0 \\ 0 \end{bmatrix}, \quad \mathbf{P}_{5} = \begin{bmatrix} 0 \\ 0 \\ 0 \\ 0 \end{bmatrix}, \quad \mathbf{P}_{5} = \begin{bmatrix} 0 \\ 0 \\ 0 \\ 0 \end{bmatrix}, \quad \mathbf{P}_{5} = \begin{bmatrix} 0 \\ 0 \\ 0 \\ 0 \end{bmatrix}, \quad \mathbf{P}_{5} = \begin{bmatrix} 0 \\ 0 \\ 0 \\ 0 \end{bmatrix}, \quad \mathbf{P}_{5} = \begin{bmatrix} 0 \\ 0 \\ 0 \\ 0 \end{bmatrix}, \quad \mathbf{P}_{5} = \begin{bmatrix} 0 \\ 0 \\ 0 \\ 0 \end{bmatrix}, \quad \mathbf{P}_{5} = \begin{bmatrix} 0 \\ 0 \\ 0 \\ 0 \end{bmatrix}, \quad \mathbf{P}_{5} = \begin{bmatrix} 0 \\ 0 \\ 0 \\ 0 \end{bmatrix}, \quad \mathbf{P}_{5} = \begin{bmatrix} 0 \\ 0 \\ 0 \\ 0 \end{bmatrix}, \quad \mathbf{P}_{5} = \begin{bmatrix} 0 \\ 0 \\ 0 \\ 0 \end{bmatrix}, \quad \mathbf{P}_{5} = \begin{bmatrix} 0 \\ 0 \\ 0 \\ 0 \end{bmatrix}, \quad \mathbf{P}_{5} = \begin{bmatrix} 0 \\ 0 \\ 0 \\ 0 \end{bmatrix}, \quad \mathbf{P}_{5} = \begin{bmatrix} 0 \\ 0 \\ 0 \\ 0 \end{bmatrix}, \quad \mathbf{P}_{5} = \begin{bmatrix} 0 \\ 0 \\ 0 \\ 0 \end{bmatrix}, \quad \mathbf{P}_{5} = \begin{bmatrix} 0 \\ 0 \\ 0 \\ 0 \end{bmatrix}, \quad \mathbf{P}_{5} = \begin{bmatrix} 0 \\ 0 \\ 0 \\ 0 \end{bmatrix}, \quad \mathbf{P}_{5} = \begin{bmatrix} 0 \\ 0 \\ 0 \\ 0 \end{bmatrix}, \quad \mathbf{P}_{5} = \begin{bmatrix} 0 \\ 0 \\ 0 \\ 0 \end{bmatrix}, \quad \mathbf{P}_{5} = \begin{bmatrix} 0 \\ 0 \\ 0 \\ 0 \end{bmatrix}, \quad \mathbf{P}_{5} = \begin{bmatrix} 0 \\ 0 \\ 0 \\ 0 \end{bmatrix}, \quad \mathbf{P}_{5} = \begin{bmatrix} 0 \\ 0 \\ 0 \\ 0 \end{bmatrix}, \quad \mathbf{P}_{5} = \begin{bmatrix} 0 \\ 0 \\ 0 \\ 0 \end{bmatrix}, \quad \mathbf{P}_{5} = \begin{bmatrix} 0 \\ 0 \\ 0 \\ 0 \end{bmatrix}, \quad \mathbf{P}_{5} = \begin{bmatrix} 0 \\ 0 \\ 0 \\ 0 \end{bmatrix}, \quad \mathbf{P}_{5} = \begin{bmatrix} 0 \\ 0 \\ 0 \\ 0 \end{bmatrix}, \quad \mathbf{P}_{5} = \begin{bmatrix} 0 \\ 0 \\ 0 \\ 0 \end{bmatrix}, \quad \mathbf{P}_{5} = \begin{bmatrix} 0 \\ 0 \\ 0 \\ 0 \end{bmatrix}, \quad \mathbf{P}_{5} = \begin{bmatrix} 0 \\ 0 \\ 0 \\ 0 \end{bmatrix}, \quad \mathbf{P}_{5} = \begin{bmatrix} 0 \\ 0 \\ 0 \\ 0 \end{bmatrix}, \quad \mathbf{P}_{5} = \begin{bmatrix} 0 \\ 0 \\ 0 \\ 0 \end{bmatrix}, \quad \mathbf{P}_{5} = \begin{bmatrix} 0 \\ 0 \\ 0 \\ 0 \end{bmatrix}, \quad \mathbf{P}_{5} = \begin{bmatrix} 0 \\ 0 \\ 0 \\ 0 \end{bmatrix}, \quad \mathbf{P}_{5} = \begin{bmatrix} 0 \\ 0 \\ 0 \\ 0 \end{bmatrix}, \quad \mathbf{P}_{5} = \begin{bmatrix} 0 \\ 0 \\ 0 \\ 0 \end{bmatrix}, \quad \mathbf{P}_{5} = \begin{bmatrix} 0 \\ 0 \\ 0 \\ 0 \end{bmatrix}, \quad \mathbf{P}_{5} = \begin{bmatrix} 0 \\ 0 \\ 0 \\ 0 \end{bmatrix}, \quad \mathbf{P}_{5} = \begin{bmatrix} 0 \\ 0 \\ 0 \\ 0 \end{bmatrix}, \quad \mathbf{P}_{5} = \begin{bmatrix} 0 \\ 0 \\ 0 \\ 0 \end{bmatrix}, \quad \mathbf{P}_{5} = \begin{bmatrix} 0 \\ 0 \\ 0 \\ 0 \end{bmatrix}, \quad \mathbf{P}_{5} = \begin{bmatrix} 0 \\ 0 \\ 0 \\ 0 \end{bmatrix}, \quad \mathbf{P}_{5} = \begin{bmatrix} 0 \\ 0 \\ 0 \\ 0 \end{bmatrix}, \quad \mathbf{P}_{5} = \begin{bmatrix} 0 \\ 0 \\ 0 \\ 0 \end{bmatrix}, \quad \mathbf{P}_{5} = \begin{bmatrix} 0 \\ 0 \\ 0 \\ 0 \end{bmatrix}, \quad \mathbf{P}_{5} = \begin{bmatrix} 0 \\ 0 \\ 0 \\ 0 \end{bmatrix}, \quad \mathbf{P}_{5} = \begin{bmatrix} 0 \\ 0 \\ 0 \\ 0 \end{bmatrix}, \quad \mathbf{P}_{5} = \begin{bmatrix} 0 \\ 0 \\ 0 \\$$

where  $\mathbf{q}$  is the vector of conserved variables,  $\mathbf{E}_a$ ,  $\mathbf{F}_a$  and  $\mathbf{G}_a$  are the convective flux vectors,  $\mathbf{E}_v$ ,  $\mathbf{F}_v$  and  $\mathbf{G}_v$  are the viscous flux vectors, u, v and w are the fluid velocity, p is the fluid pressure and Re is Reynolds number. The equations are nondimensionalized by

$$x = \frac{\overline{x}}{\overline{L}_0}, \quad y = \frac{\overline{y}}{\overline{L}_0}, \quad z = \frac{\overline{z}}{\overline{L}_0}, \quad u = \frac{\overline{u}}{\overline{U}_0}, \quad v = \frac{\overline{v}}{\overline{U}_0}, \quad w = \frac{\overline{w}}{\overline{U}_0}, \quad p = \frac{\overline{p}}{\overline{\rho}\overline{U}_0^2}, \quad t = \frac{\overline{t}}{\overline{L}_0/\overline{U}_0}, \quad \text{Re} = \frac{\overline{\rho}\overline{L}_0\overline{U}_0}{\overline{\mu}},$$

where overline shows the dimensional quantity,  $\overline{L}_0$  is the characteristics length,  $\overline{U}_0$  is the characteristics velocity,  $\overline{\rho}$  is the characteristics density and  $\overline{\mu}_0$  is the viscosity.

#### Discretization

In Moving-Grid Finite-Volume Method (MGFVM) is used for discretization. In MGFVM, the control volume in the space-time unified four-dimensional (x, y, z, t) domain is used in order to assure both physical and geometrical conservation laws simultaneously. Fig. 1 shows the Unstructured computational cell on three-dimensional (x, y, z) domain at m time step and m+1 time step.  $\mathbf{R} = (x, y, z)^T$ , the subscript i shows the computational grid number and the superscript m shows time step. In four-dimensional domain, the blue computational cell is the surface (l = 5) perpendicular to t-axis at m time step and the red computational cell is the surface (l = 6) perpendicular to t-axis at m+1 time step. The control volume  $\Omega$  is a volume on four-dimensional domain and formed between the lower surface (l = 5) and the upper surface (l = 6). The control surface is the surface of the control volume on a unified four-dimensional space-time (x, y, z, t) domain and corresponds the volume on three-dimensional domain. The control surface is formed by the surface at m time step and it at m+1 time step  $(l = 1, 2, \dots, 4)$ , corresponds the computational cell at m time step (l = 6). For example, the control surface l = 4 corresponds the volume on three-dimensional domain shown by the heavy line in Fig. 2.

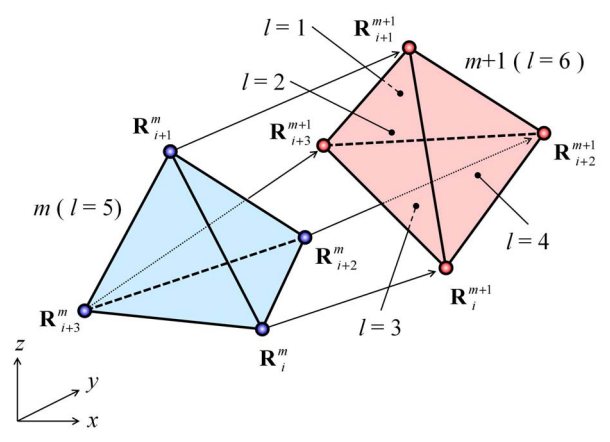


Figure 1. Computational cells at *m* time step and *m*+1 time step

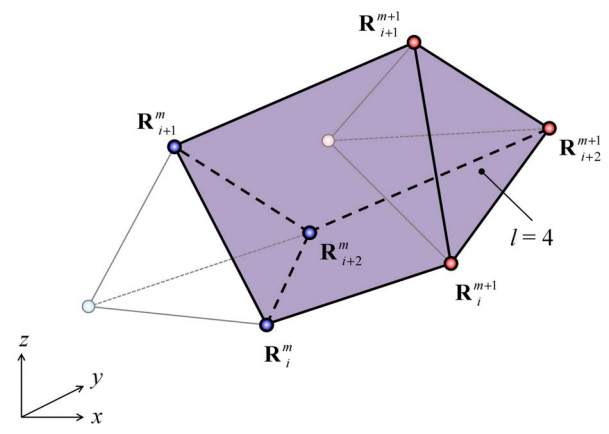


Figure 2. Control surface l = 4

Navier-Stokes equations for incompressible flows are discretized with Unstructured Moving-Grid Finite-Volume Method. Eq.(2) is integrated over the control volume  $\Omega$  as

$$\int_{\Omega} \left[ \frac{\partial (\mathbf{E} + \mathbf{P}_1)}{\partial x} + \frac{\partial (\mathbf{F} + \mathbf{P}_2)}{\partial y} + \frac{\partial (\mathbf{G} + \mathbf{P}_3)}{\partial z} + \frac{\partial \mathbf{q}}{\partial t} \right] d\Omega = \mathbf{0}.$$
 (3)

Eq.(3) is shown in divergence as

$$\int_{\Omega} \left[ \left( \frac{\partial}{\partial x}, \frac{\partial}{\partial y}, \frac{\partial}{\partial z}, \frac{\partial}{\partial t} \right) \left\{ (\mathbf{E} + \mathbf{P}_1), (\mathbf{F} + \mathbf{P}_2), (\mathbf{G} + \mathbf{P}_3), \mathbf{q} \right\} \right] d\Omega = \mathbf{0}.$$
 (4)

Gauss' divergence theorem is applied to four-dimensional domain and Eq.(4) becomes as follows:

$$\sum_{l=1}^{6} \left\{ \left( \mathbf{E} + \mathbf{P}_{1} \right) \widetilde{n}_{x} + \left( \mathbf{F} + \mathbf{P}_{2} \right) \widetilde{n}_{y} + \left( \mathbf{G} + \mathbf{P}_{3} \right) \widetilde{n}_{z} + \mathbf{q} \widetilde{n}_{t} \right\}_{l} S_{l} = \mathbf{0},$$
 (5)

Therefore Eq.(5) becomes as follows:

$$\mathbf{q}^{m+1}V^{m+1} - \mathbf{q}^{m}V^{m} + \sum_{l=1}^{4} \left\{ \mathbf{q}^{m+1/2} \widetilde{n}_{t} + \left(\mathbf{E} + \mathbf{P}_{1}\right)^{m+1/2} \widetilde{n}_{x} + \left(\mathbf{F} + \mathbf{P}_{2}\right)^{m+1/2} \widetilde{n}_{y} + \left(\mathbf{G} + \mathbf{P}_{3}\right)^{m+1/2} \widetilde{n}_{z} \right\}_{l} S_{l} = 0.$$
 (6)

This equation is the fundamental equation of Unstructured Moving-Grid Finite-Volume Method.

Fractional Step Method

By fractional step method, Eq.(6) is divided as 1st step:

$$\mathbf{q}^* V^{m+1} - \mathbf{q}^m V^m + \frac{1}{2} \left[ \sum_{l=1}^4 \left\{ \left( \mathbf{q}^* + \mathbf{q}^m \right) \widetilde{n}_t + \left( \mathbf{E}^* + \mathbf{E}^m \right) \widetilde{n}_x + \left( \mathbf{F}^* + \mathbf{F}^m \right) \widetilde{n}_y + \left( \mathbf{G}^* + \mathbf{G}^m \right) \widetilde{n}_z \right\}_l S_l \right] = 0, \tag{7}$$

2nd step:

$$\left(\mathbf{q}^{m+1} - \mathbf{q}^*\right) V^{m+1} + \sum_{l=1}^{4} \left(\mathbf{P}_1^{m+1/2} \widetilde{n}_x + \mathbf{P}_2^{m+1/2} \widetilde{n}_y + \mathbf{P}_3^{m+1/2} \widetilde{n}_z\right)_l S_l = 0,$$
(8)

where \* shows intermediate step.

The divergence of Eq.(8) on three-dimensional (x, y, z) domain at m+1 time step becomes as follows:

$$\left(D^{m+1} - D^*\right)V^{m+1} + \sum_{l=1}^{4} \left(\frac{\partial p^{m+1/2}}{\partial x^{m+1}}\widetilde{n}_x + \frac{\partial p^{m+1/2}}{\partial y^{m+1}}\widetilde{n}_y + \frac{\partial p^{m+1/2}}{\partial z^{m+1}}\widetilde{n}_z\right)_l S_l = 0,$$
(9)

with

$$D^{m+1} = \frac{\partial u^{m+1}}{\partial x^{m+1}} + \frac{\partial v^{m+1}}{\partial v^{m+1}} + \frac{\partial w^{m+1}}{\partial z^{m+1}}, D^* = \frac{\partial u^*}{\partial x^{m+1}} + \frac{\partial v^*}{\partial v^{m+1}} + \frac{\partial w^*}{\partial z^{m+1}}.$$

Here, pay attention that this is the divergence on (x, y, z) domain at m+1 time step in order to correlate to the continuity equation Eq.(1) at m+1 time step. Assuming that the continuity equation Eq.(1) is satisfied at m+1 time step  $(D^{m+1}=0)$ , Eq.(9) becomes the pressure equation including the normal vectors on four-dimensional (x, y, z, t) domain as follows:

$$-D^*V^{m+1} + \sum_{l=1}^{4} \left( \frac{\partial p^{m+1/2}}{\partial x^{m+1}} \widetilde{n}_x + \frac{\partial p^{m+1/2}}{\partial y^{m+1}} \widetilde{n}_y + \frac{\partial p^{m+1/2}}{\partial z^{m+1}} \widetilde{n}_z \right)_l S_l = 0, \tag{10}$$

where the differential of pressure on three-dimensional (x, y, z) domain at m+1 time step is solved with finite-volume-method on the computational cell at m+1 time step.

The computational procedure is as follows:

- 1.  $q^*$  is calculated from  $q^m$  by Eq.(7).
- 2.  $p^{m+1/2}$  is calculated from  $q^*$  by Eq.(10). 3.  $q^{m+1}$  is calculated from  $q^*$  and  $p^{m+1/2}$  by Eq.(8).

## Other Numerical Method

The convective flux vectors ( $\mathbf{E}_a$ ,  $\mathbf{F}_a$ ,  $\mathbf{G}_a$ ) are evaluated with second order upwind difference scheme. The viscous flux vectors  $(\mathbf{E}_{\nu}, \mathbf{F}_{\nu}, \mathbf{G}_{\nu})$  and the pressure vectors  $(\mathbf{P}_{1}, \mathbf{P}_{2}, \mathbf{P}_{3})$  are evaluated with central difference scheme. The iterative method of Eq.(7) is LU-SGS [Yoon and Jameson (1988)] and the iterative method of Eq.(10) is Bi-CGSTAB [van der Vorst (1992)].

#### **Numerical methods for body motion**

### Governing Equation

The governing equations of body-motion are Newton's motion equation with six degrees of freedom of motion including translation and rotation as follows:

$$\frac{d}{dt} \begin{bmatrix} Mu_B \\ Mv_B \\ Mw_B \end{bmatrix} = \begin{bmatrix} F_x \\ F_y \\ F_z - Mg \end{bmatrix},$$
(11)

$$\frac{d}{dt} \begin{bmatrix} x_B \\ y_B \\ z_B \end{bmatrix} = \begin{bmatrix} u_B \\ v_B \\ w_B \end{bmatrix},\tag{12}$$

$$\frac{d}{dt} \begin{bmatrix} I_x \omega_x \\ I_y \omega_y \\ I_z \omega_z \end{bmatrix} + \begin{bmatrix} (I_z - I_y) \omega_z \omega_y \\ (I_x - I_z) \omega_x \omega_z \\ (I_y - I_x) \omega_y \omega_x \end{bmatrix} = \begin{bmatrix} T'_x \\ T'_y \\ T'_z \end{bmatrix}, \tag{13}$$

where M is the weight of the body,  $u_B$ ,  $v_B$  and  $w_B$  are the body velocity,  $F_x$ ,  $F_y$  and  $F_z$  are the forces to be received by the fluid, g is gravity acceleration,  $I_x$ ,  $I_y$  and  $I_z$  are the moment of inertia of the body about a center of x', y' and z' axis,  $\omega_x$ ,  $\omega_y$  and  $\omega_z$  are the body angle speed about a center of x', y' and z' axis,  $T_x$ ,  $T_y$  and  $T_z$  are the torques to be received by the fluid about a center of x', y' and z' axis and (x', y', z') is the cartesian coordinate fixed to the body. The equations are nondimensionalized by

$$\begin{split} M &= \frac{\overline{M}}{\overline{\rho}\overline{L}_0^3}, \quad u_B = \frac{\overline{u}_B}{\overline{U}_0}, \quad v_B = \frac{\overline{v}_B}{\overline{U}_0}, \quad w_B = \frac{\overline{w}_B}{\overline{U}_0}, \quad F_x = \frac{\overline{F}_x}{\overline{\rho}\overline{U}_0^2/\overline{L}_0^2}, \quad F_y = \frac{\overline{F}_y}{\overline{\rho}\overline{U}_0^2/\overline{L}_0^2}, \quad F_z = \frac{\overline{F}_z}{\overline{\rho}\overline{U}_0^2/\overline{L}_0^2}, \\ g &= \frac{\overline{g}}{\overline{U}_0^2/\overline{L}_0}, \quad I_x = \frac{\overline{I}_x}{\overline{\rho}\overline{L}_0}, \quad I_y = \frac{\overline{I}_y}{\overline{\rho}\overline{L}_0}, \quad I_z = \frac{\overline{I}_z}{\overline{\rho}\overline{L}_0}, \quad \omega_x = \frac{\overline{\omega}_x}{\overline{U}_0/\overline{L}_0}, \quad \omega_y = \frac{\overline{\omega}_y}{\overline{U}_0/\overline{L}_0}, \quad \omega_z = \frac{\overline{\omega}_z}{\overline{U}_0/\overline{L}_0}, \\ T_x &= \frac{\overline{T}_x}{\overline{\rho}\overline{U}_0^2/\overline{L}_0}, \quad T_y = \frac{\overline{T}_y}{\overline{\rho}\overline{U}_0^2/\overline{L}_0}, \quad T_z = \frac{\overline{T}_z}{\overline{\rho}\overline{U}_0^2/\overline{L}_0}, \end{split}$$

where overline shows the dimensional quantity. Quaternion [Yatabe (2007)] is used for the coordinate transform.

The time derivative of Eq.(11) and (13) is discretized by forward Euler method and the time derivative of Eq.(12) is discretized by Crank-Nicolson method as follows:

$$\begin{cases}
Mu_{B}^{m+1} = Mu_{B}^{m} + F_{x}^{m} \Delta t \\
Mv_{B}^{m+1} = Mv_{B}^{m} + F_{y}^{m} \Delta t \\
Mw_{B}^{m+1} = Mw_{B}^{m} + (F_{z}^{m} - Mg) \Delta t
\end{cases} (14)$$

$$\begin{cases} x_B^{m+1} = x_B^m + 0.5 \left( u_B^{m+1} + u_B^m \right) \Delta t \\ y_B^{m+1} = y_B^m + 0.5 \left( v_B^{m+1} + v_B^m \right) \Delta t \\ z_B^{m+1} = z_B^m + 0.5 \left( w_B^{m+1} + w_B^m \right) \Delta t \end{cases}$$
(15)

$$\begin{cases}
I_{x}\omega_{x}^{m+1} = \omega_{x}^{m} + \left(T_{x}^{m} - \left(I_{z} - I_{y}\right)\omega_{z}^{m}\omega_{y}^{m}\right)\Delta t \\
I_{y}\omega_{y}^{m+1} = \omega_{y}^{m} + \left(T_{y}^{m} - \left(I_{x} - I_{z}\right)\omega_{x}^{m}\omega_{z}^{m}\right)\Delta t \\
I_{z}\omega_{z}^{m+1} = \omega_{z}^{m} + \left(T_{z}^{m} - \left(I_{y} - I_{z}\right)\omega_{y}^{m}\omega_{z}^{m}\right)\Delta t
\end{cases} \tag{16}$$

Coupled Procedure of Fluid-Flow and Body-Motion

The computational procedure is as follows:

- 1. The force and the torque of the body at *m* time step are calculated from the pressure and the shear stress of the fluid.
- 2. The velocity and the angle speed of the body at m+1 time step are calculated by Eq.(14) and Eq.(16).
- 3. The translation and the rotation of the body at m+1 time step are calculated by Eq.(15) and quaternion.
- 4. The computational grid at m+1 time step is formed.
- 5. The velocity and the pressure of the fluid at m+1 time step are calculated by Eq.(7), Eq.(8) and Eq.(10).

## **Numerical simulation**

### Computational Condition

Fig. 3 shows the jellyfish which is the target of this simulation. The jellyfish is 16.8-24.0mm in diameter DB, 8.64-12.48mm in height HB, 1mm in thickness, 10g in weight and elliptical cross section. The water is  $1000 \text{kg/m}^3$  in density and  $1.0*10^{-3} \text{kg/ms}$  in viscosity.  $\overline{L}_0$  is 24.0mm,  $\overline{U}_0$  is 24.0mm/s,  $\overline{\rho}$  is  $1000 \text{kg/m}^3$ ,  $\overline{\mu}_0$  is  $1.0*10^{-3} \text{kg/ms}$ , Re is 576, M is 10g and g is  $0.0 \text{m/s}^2$  considering buoyancy. Case1 is condition without a current and Case2 is condition with a current. The jellyfish velocity  $(u_B, v_B, w_B)$  is (0.0, 0.0, 0.0) in the initial condition. The change of diameter DB and height HB is decided as follows:

$$\begin{cases}
\frac{DB}{\overline{L}_{0}} = 1.0 - 0.3 \exp\left(-Ln\left(\frac{[t \mod 1.12]}{0.44}\right)^{2} / 0.15\right) \\
\frac{HB}{\overline{L}_{0}} = 0.36 - 0.16 \exp\left(-Ln\left(\frac{[t \mod 1.12]}{0.44}\right)^{2} / 0.15\right)
\end{cases} (14)$$

Fig.4 shows time history of diameter DB and height HB, where Exp denotes the experimental data [Mchenry and Jed (2003)].

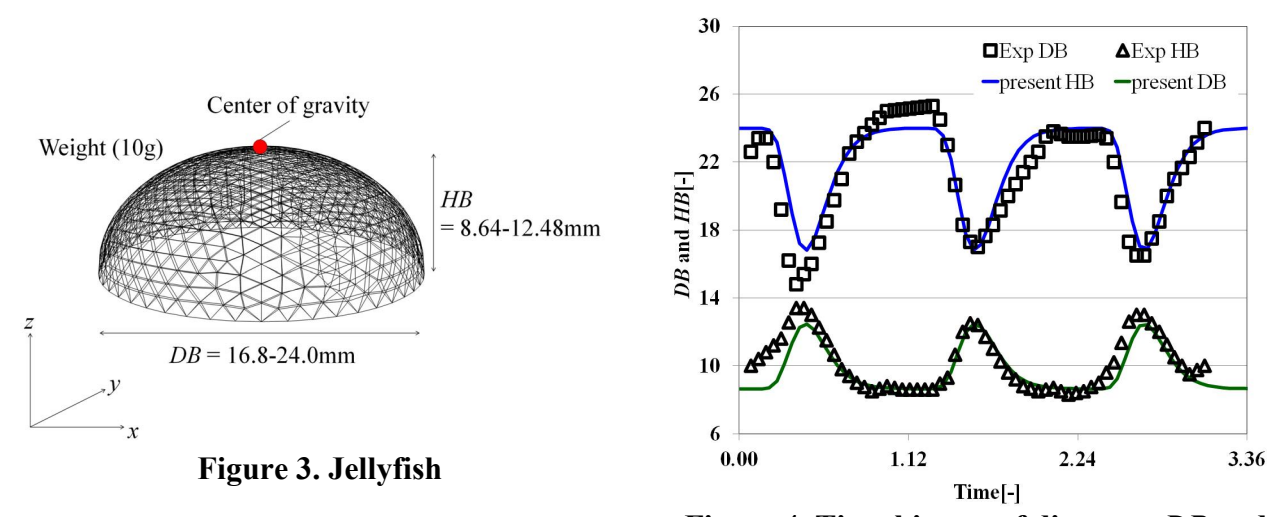


Figure 4. Time history of diameter *DB* and height *HB*.

Fig. 5 shows the computational domain and the boundary conditions. The computational domain is a sphere 240mm in diameter. In BC1 which is the wall boundary of the jellyfish, the velocity is fixed to the velocity of the jellyfish and Neumann boundary condition applies to the pressure. In BC2 which is the external boundary, the inflow velocity is fixed to (u, v, w) = (ui, vi, wi), the outflow velocity is calculated by linear interpolation and Neumann boundary condition applies to the pressure. The whole of computational grid moves together with the jellyfish by using Moving Computational Domain (MCD) approach [Watanabe and Matsuno (2009)]. Simulations are performed in three conditions Case1, Case2 and Case3 as shown in Table 1.

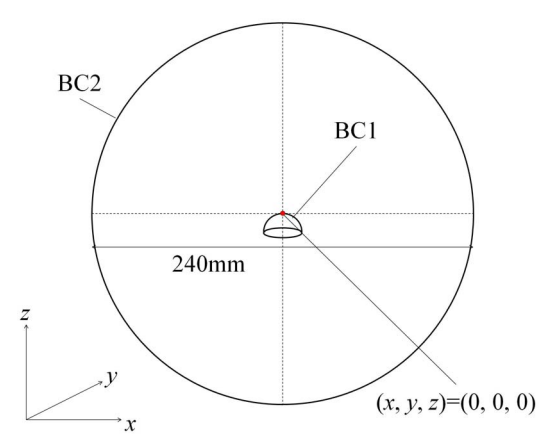


Figure 5. Computational domain and boundary conditions

**Table 1. Conditions of simulation** 

	Case1	Case2	Case3
Current	Without	With	With
(ui, vi, wi)	(0.0, 0.0, 0.0)	(0.5, 0.0, 0.0)	(0.5, 0.0, 0.0)
Diameter DB	Eq.(14)	Eq.(14)	Constant (24.0mm)
Height HB	Eq.(14)	Eq.(14)	Constant (8.64mm)

## Result of Simulation

As a result, Fig. 6, 7 and 8 each show velocity vectors, pressure contours and vorticity magnitude contours in Case1 at t = 0.40 (contraction) and t = 1.12 (relaxation). Colors denote magnitude velocity in Fig. 6. The contour denotes 4.0 of vorticity magnitude in Fig. 8. The starting vortex occurs outside the jellyfish at the contraction and the stopping vortex occurs inside the jellyfish at the relaxation. The whole flow field is axisymmetric.

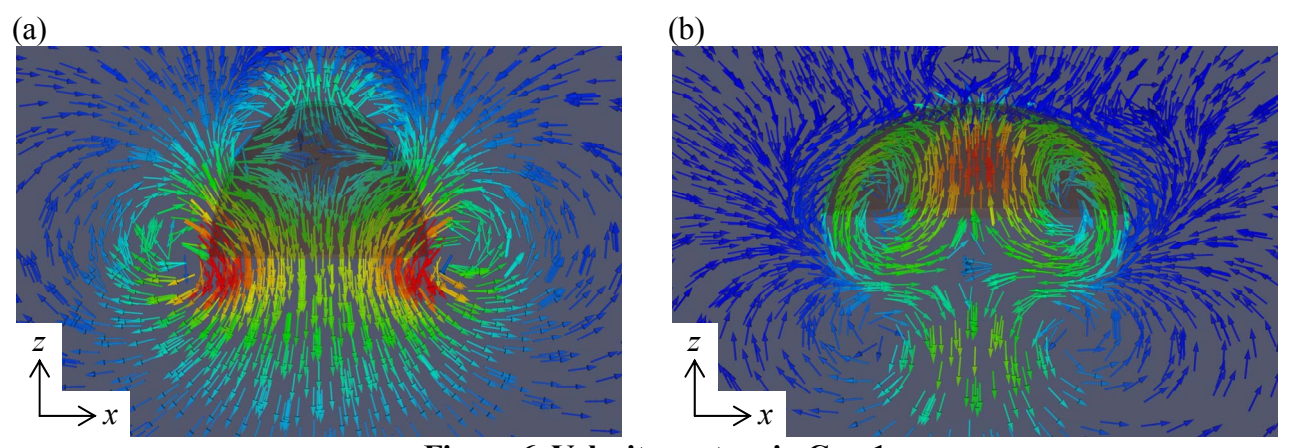


Figure 6. Velocity vectors in Case1 at (a) t = 0.40 (contraction) and (b) t = 1.12 (relaxation)

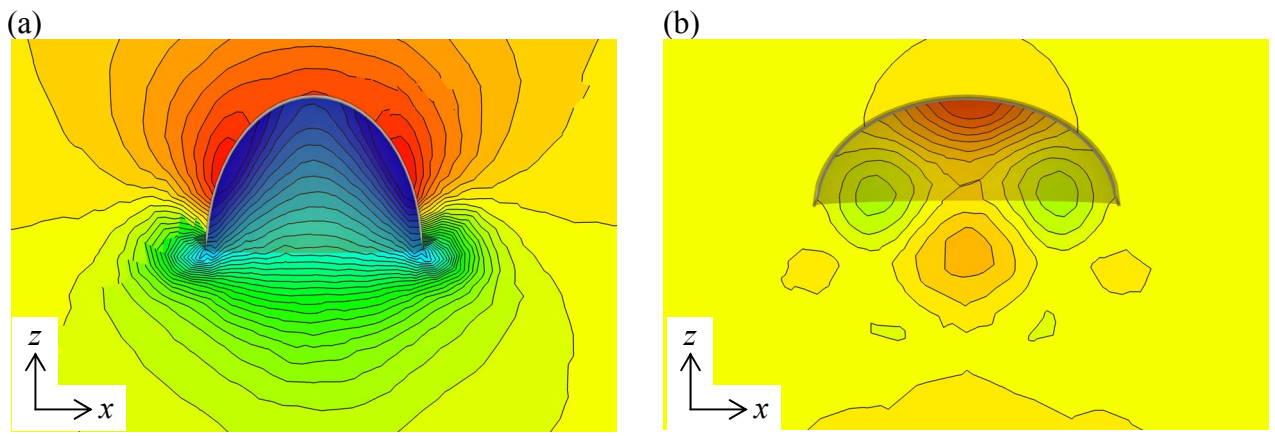


Figure 7. Pressure contours in Case1 at (a) t = 0.40 (contraction) and (b) t = 1.12 (relaxation)

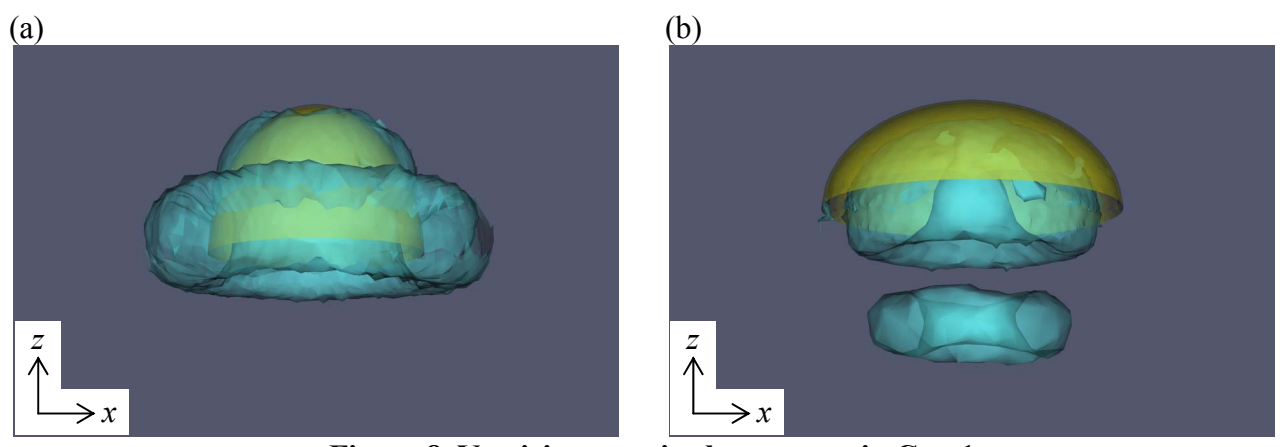


Figure 8. Vorticity magnitude contours in Case1 at (a) t = 0.40 (contraction) and (b) t = 1.12 (relaxation)

Fig. 9 shows swimming speed  $w_B$  of the jellyfish in Case1, where Exp denotes experimental result [Mchenry and Jed (2003)]. The jellyfish accelerates at the contraction and decelerates at relaxation. The present result gives good agreement with experimental result.

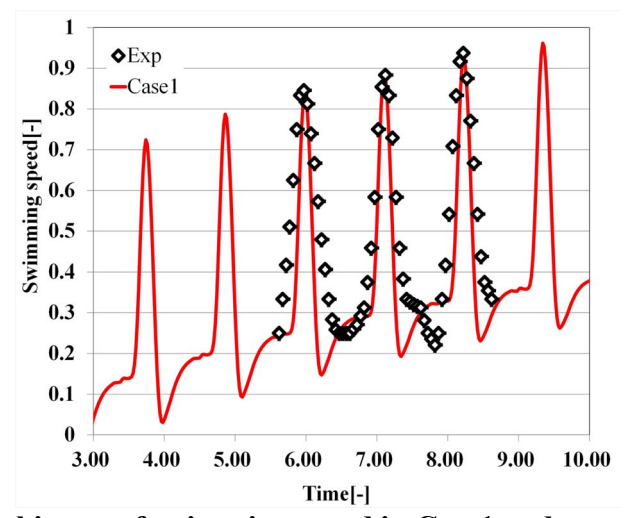


Figure 9. Time history of swimming speed in Case1 and experimental result

Fig. 10, 11 and 12 each show velocity vectors, pressure contours and vorticity magnitude contours in Case2 at t = 0.40 (contraction) and t = 1.12 (relaxation). Colors denote magnitude velocity in Fig. 10. The contour denotes 4.0 of vorticity magnitude in Fig. 12. The flow field is not axisymmetric because of the current. At relaxation, the stopping vortex is clear not vortex structure in the right side and pressure in the jellyfish is higher in the right side. The asymmetry of the vortex structure inclines the jellyfish to x-axis negative direction.

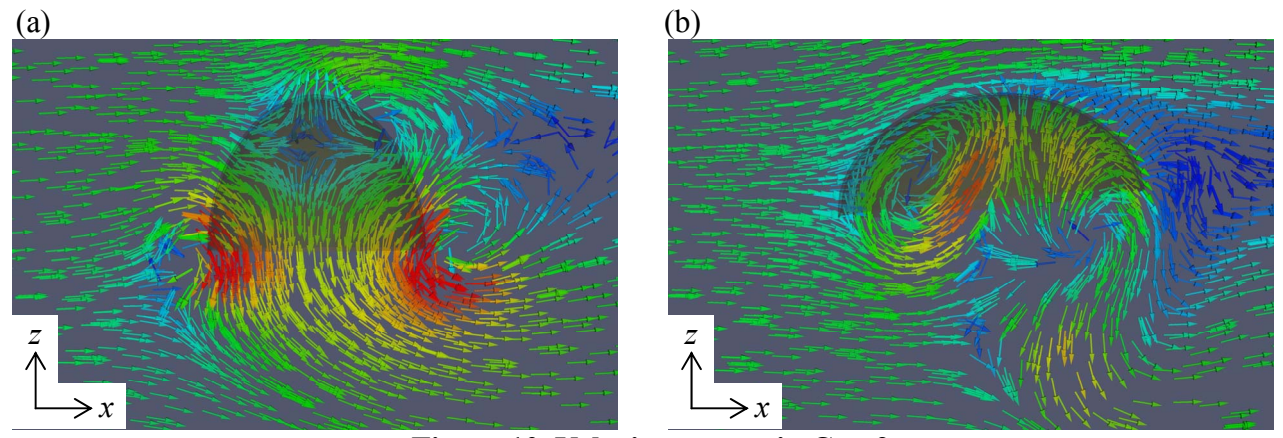


Figure 10. Velocity vectors in Case2 at (a) t = 0.40 (contraction) and (b) t = 1.12 (relaxation)

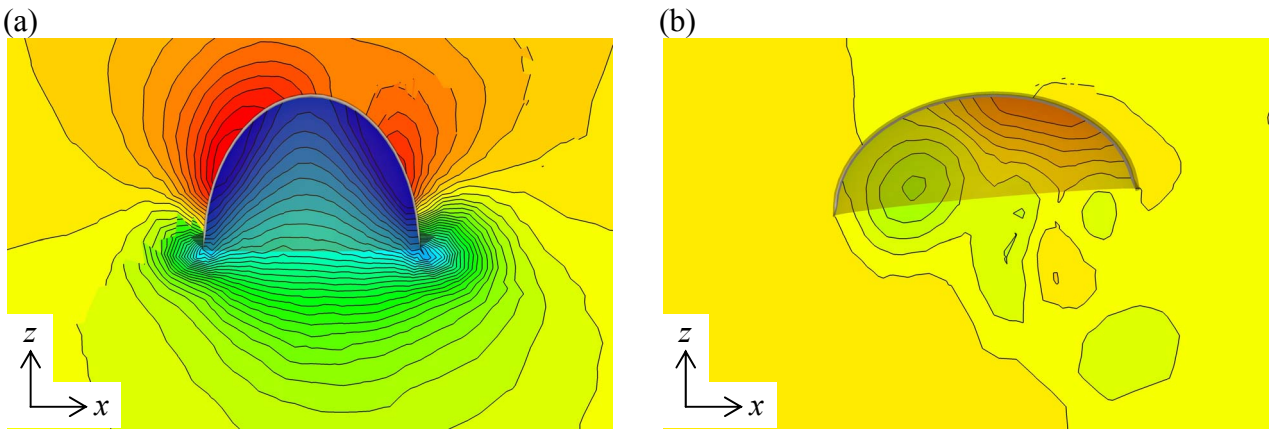


Figure 11. Pressure contours in Case2 at (a) t = 0.40 (contraction) and (b) t = 1.12 (relaxation)

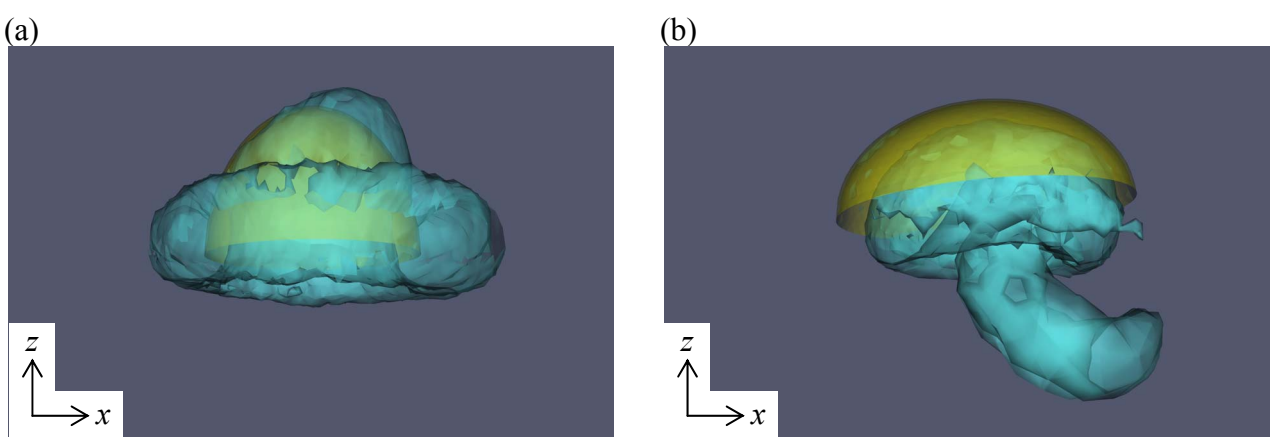


Figure 12. Vorticity magnitude contours in Case2 at (a) t = 0.40 (contraction) and (b) t = 1.12 (relaxation)

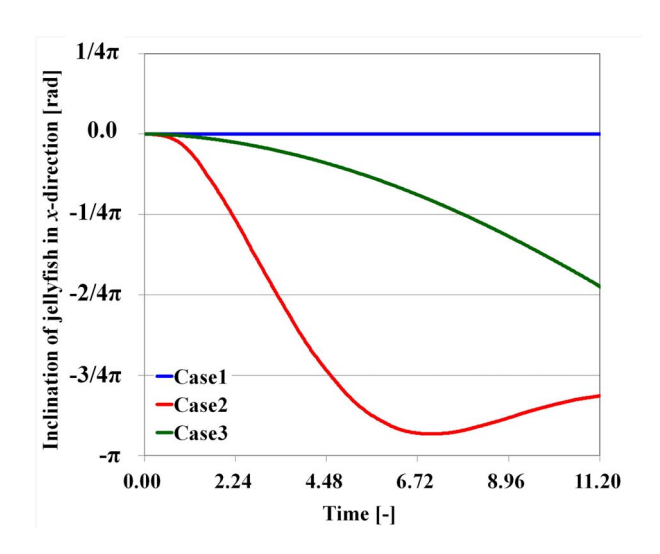


Figure 13. Time history of inclination angle of jellyfish in x-direction in Case1 (blue line), Case2 (red line) and Case3 (green line)

Fig. 13 shows time history of the inclination angle of the jellyfish in x-direction. In Case1 without a current and with the contraction motion, the jellyfish does not rotate because the whole flow field is axisymmetric, and the inclination angle is almost zero. In Case3 with a current and without the contraction motion, the current itself rotates the jellyfish to x-axis negative direction, and the inclination angle decreases gradually. In Case2 with a current and the contraction motion, moreover the vortex structure which becomes asymmetric by the current rotates the jellyfish to x-axis negative direction, and the inclination angle decreases faster than Case3.

### **CONCLUTIONS**

In this paper, we have performed three-dimensional coupled simulation of fluid-flow and jellyfish-swimming in a current with six degrees of freedom of motion by using Moving-Grid Finite-Volume Method. In the simulation without a current, the jellyfish accelerates at the contraction and decelerates at relaxation. The swimming speed of the jellyfish gave good agreement with experimental result. Moreover, in the simulation with a current, the current makes flow field asymmetric and changes the vortex structure caused by swimming jellyfish. The vortex structure rotates swimming jellyfish.

#### References

Inomoto, T. Matsuno, K. and Yamakawa, M. (2004) A moving-grid finite-volume method for three-dimensional incompressible flows, *Proceedings of JSFM 18th Computational Fluid Dynamics Symposium*, D2-3.

Mihara, K., Matsuno, K. and Satofuka, N. (1999) An iterative finite-volume scheme on a moving grid (1st report, The fundamental formulations and validation), *Transactions of the Japan Society of Mechanical Engineers*, Series B, Vol.65, No.637, 2945-2953.

Matsuno, K. (2001) A moving mesh finite-volume scheme for compressible flows, *Computational Fluid Dynamics 2000*, Springer, 705-710. (*Proceedings of 1st International Conference on Computational Fluid Dynamics 2000*, Kyoto, Japan, July, 2000)

Matsuno, K. (2010) Developments and Applications in Engineering Computational Technology, Saxe-Coburg Publications, 103-127.

Noh, W. F. (1964) A time-dependent, two space dimensional, coupled Eulerian-Lagrange code, *Methods in Computational Physics*, **3**, 117-179.

Tezduyar, T. E., Behr, M. and Liou, J. (1992) A new strategy for finite element computations involving moving boundaries and interfaces - the deforming-spatial-domain/space-time procedure: I. The concept and preliminary numerical tests, *Computer Methods in Applied Mechanics and Engineering*, **94**, 339-351.

Thomas, P. D. and Lombard, C. K. (1979) Geometric conservation law and its application to flow computations on moving grids, *AIAA Journal*, **17**-10, 1030-1037.

- van der Vorst, H.A. (1992) Bi-CGSTAB: A fast and smoothly converging variant of Bi-CG for the solution of nonsymmetric linear systems, SIAM Journal on Scientific and Satistical Computing, 13-2, 631-644.
- Vinokur, M. (1974) Conservation equations of gasdynamics in curvilinear coordinate systems, *Journal of Computational Physics*, **14**-2, 105-125.
- Watanabe, K. and Matsuno, K. (2009) Moving computational domain method and its application to flow around a high-speed car passing through a hairpin curve, *Journal of computational Science and Technology*, **3-**2, 449-459.
- Yamakawa, M. and Matsuno, K. (2003) An iterative finite-volume method on an unstructured moving grid (1st report, the fundamental formulation and validation for unsteady compressible flows), *Transactions of the Japan Society of Mechanical Engineers*, Series B, **69**-683, 1577-1582.
- Yatabe, M. (2007) Handy Note for Quaternion, MSS, 18, 29-34.
- Yoon, S. and Jameson, A. (1988) Lower-upper Symmetric-Gauss-Seidel method for the Euler and Navier-Stokes equations, *AIAA Journal*, **26**-9, 1025-1026.
- Costello, J. H., Colin, S. P. and Dabiri, J. O. (2008) Medusan morphospace: phylogenetic contrants, biomechanical solutions, and ecological consequences, *Invertebrate Biology*, **127**, 265–290.
- Colin, S. P. and Costello, J. H. (2002) Morphology, swimming performance and propulsive mode of six co-occurring hydromedusae. *Journal of Experimental Biology*, **205**, 427–437.
- Mchenry, M. J. and Jed, J. (2003) The ontogenetic scaling of hydrodynamics and swimming performance in jellyfish (Aurelia aurita), *Journal of Experimental Biology*, **206**, 4125–4137.
- Dabiri, J. O., Colin, S. P., Costello, J. H. and Gharib, M. (2005) Flow patterns generated by oblate medusa jellyfish: field measurements and laboratory analyses, *Journal of Experimental Biology*, **208**, 1257–1265.
- Dular, M., Bajcar, T. and Sirok, B. (2009) Numerical investigation of flow in the vicinity of a swimming jellyfish, *Engineering Applications of Computational Fluid Mechanics*, **3**, 258–270.
- Sahin, M. and Mohseni, K. (2009) An arbitrary Lagrangian–Eulerian formulation for the numerical simulation of flow patterns generated by the hydromedusa Aequorea victoria, *Journal of Computational Physics*, **228**, 4588–4605.
- Alben, S., Miller, L. A. and Peng, J. (2013) Efficient kinematics for jet-propelled swimming, *Journal of Fluid Mechanics*, **733**, 100–133.
- Rudolf, D. and Mould, D. (2010) An interactive fluid model of jellyfish for animation, *Communications in Computer and Information Science*, **68**, 59–72.